Protoplasma (2004) 223: 155–162
DOI 10.1007/s00709-003-0033-3

PROTOPLASMA
Printed in Austria

Use of energy-filtering transmission electron microscopy for routine ultrastructural analysis of high-pressure-frozen or chemically fixed plant cells

U. Lütz-Meindl* and **N. Aichinger**

Institute of Plant Physiology, University of Salzburg, Salzburg

Received August 14, 2003; accepted September 30, 2003; published online April 21, 2004

Summary. In the present study energy-filtering transmission electron microscopy by use of an in-column spectrometer is employed as a powerful tool for ultrastructural analysis of plant cells. Images of unstained very thin (50 nm) and thick (140 nm) sections of the unicellular green alga *Micrasterias denticulata,* as a model system for a growing plant cell, taken by conventional transmission electron microscopy are compared to those obtained from filtering at zero energy loss (elastic bright field) and to those generated by energy filtering below the carbon-specific absorption edge at about 250 eV. The results show that the high-contrast images produced by the latter technique are distinctly superior in contrast and information content to micrographs taken at conventional transmission electron microscopy mode or at elastic bright field. Post- or en bloc staining with heavy metals, which is indispensable for conventional bright-field transmission electron microscopy, can be completely omitted. Delicate structural details such as membranous or filamentous connections between organelles, organelle interactions, or vesicle and vacuole contents are clearly outlined against the cytoplasmic background. Also, immunoelectron microscopic localization of macromolecules benefits from energy-filtering transmission electron microscopy by a better and more accurate assignment of antigens and structures and by facilitating the detection of immunomarkers without renunciation of contrast.

Keywords: Cryofixation; Electron spectroscopic imaging; Energy filtering; Immunoelectron microscopy; *Micrasterias denticulata*; Organelle connection.

Abbreviations: CTEM conventional transmission electron microscopy; EFTEM energy filtering transmission electron microscopy; HCI high contrast image; TEM transmission electron microscopy.

Introduction

Conventional transmission electron microscopy (CTEM) essentially depends on sufficient elastic scattering of electrons at the specimen, which for biological objects consisting mainly of light elements requires staining with heavy metals like uranyl acetate and lead citrate for contrast generation. On the one hand, this means that the appearance of the structures under investigation varies with concentration, nature, and duration of the heavy metal treatment used. On the other hand, structural details may be covered by relatively unspecific accumulation of heavy metals to different cell constituents and the possibilities for obtaining high-resolution information are limited (Carlemalm et al. 1985). Immunoreactions for localization of macromolecules may be influenced or prevented by heavy metals and the detection of gold particles or other markers is impeded. However, when omitting the staining, assignment of the antigen in question to structural details is difficult. The problems arising from these facts are independent from fixation and embedding procedures. Even high-pressure freeze fixation and subsequent cryosubstitution lead to varying appearances, e.g., of secretory vesicles, in dependence of the heavy metals used during the preparation, and the reliability of the results is low when CTEM is employed.

In the present study in-column energy-filtering techniques in transmission electron microscopy (EFTEM) are applied for contrast generation (Reimer et al. 1990, Reimer 1995) and depiction of ultrastructural details of plant cells without heavy metal staining of the sections. Both thick (140 nm) and very thin (50 nm) sections are investigated by means of two energy-filtering methods. Elastic bright field filtered at zero loss energy (Reimer 1995) is used for general contrast enhancement by inserting a slit aperture to eliminate inelastically scattered electrons. Electron spectroscopic imaging is employed for obtaining an element-specific contrast which also pro-

* Correspondence and reprints: Institut für Pflanzenphysiologie, Universität Salzburg, Hellbrunnerstrasse 34, 5020 Salzburg, Austria.
E-mail: Ursula.Meindl@sbg.ac.at

vides information of the biochemical composition of the structure under investigation. In the latter case, carbon as the main element of biological objects is taken for imaging. Energy (250 eV) below the carbon-specific absorption edge (at 284 eV) is added to the acceleration voltage and the image is generated only by electrons which have lost energy in the range of 250 eV (energy window, 20 eV) at the object. This means that a "negative contrast" is generated with a minimum contribution from carbon and a relatively strong impact from noncarbon elements (Reimer 1995). EFTEM mainly for element mapping has been used only occasionally in biological sciences so far (Leapman et al. 1993, Hofer and Pabst 1998, Stegmann et al. 1999, Angert et al. 2000, Heinrich et al. 2000, Hoshi et al. 2001, Vannier-Santos and Lins 2001, Lechaire et al. 2002), which is at least in part due to a lack of access to TEMs equipped with spectrometers and to the fast advances in this technology in the recent years. To our knowledge, EFTEM by use of modern in-column spectrometers has not yet been employed at all for imaging and ultrastructural analysis of plant cells.

We use the green alga *Micrasterias denticulata* fixed both by cryomethods and by conventional chemical treatment as an example in this study since structural details of the cell are well known from investigations by different TEM techniques in the last decades (e.g., Kiermayer 1968, Meindl 1990, Meindl et al. 1992, Holzinger and Meindl 1997, Holzinger et al. 2000, Lütz-Meindl and Brosch-Salomon 2000, Oertel et al. 2003). Because of its extraordinary highly symmetric shape, the considerable cell size of about 200 μm, its well defined organelles with an extremely productive secretion machinery the alga represents a valuable model system for a growing plant cell (Meindl 1993). By comparison of images taken at CTEM with micrographs obtained at elastic bright field (filtered at zero loss energy) and with electron spectroscopic images taken below the carbon-specific absorption edge it is shown that EFTEM is superior to CTEM in both the generation of contrast and the structural information provided. In addition, it is demonstrated that a combination of immunoelectron microscopy and EFTEM facilitates the detection of markers without renunciation of contrast.

Material and methods

All chemicals were purchased from Sigma (St. Louis, Mo., U.S.A.), unless stated differently. *Micrasterias denticulata* cells were grown either in liquid desmid nutrient solution (Schlösser 1982) or on agar plates and were kept under a constant temperature of 20 °C and at a photoperiod of 14 h light and 10 h dark. "Desmid" medium supplemented with 0.5% or 0.75% agar was used for the preparation of semisolid agar plates. One single cell was inoculated per petri dish with a Pasteur pipette; for further cultivation, cells were subcultured every two months. For EFTEM, cells at different developmental stages were either chemically fixed following a potassium ferricyanide osmium tetroxide protocol (Meindl 1990) or were high-pressure frozen in a Balzers hyperbaric freezer (BalTec, Balzers, Liechtenstein) or a Leica EMPACT and freeze substituted in a Leica EM AFS (Leica Mikrosysteme GmbH, Vienna, Austria) freeze substitution apparatus. For high-pressure freeze fixation, cells of defined developmental stages or nongrowing interphase cells were either wrapped in cotton fibrils and placed in specimen holders of the freezing device (Meindl et al. 1992) or were frozen in their own mucilage envelope. For the latter procedure, mucilage plugs with cells were transferred from the agar plates into the sample holders by tweezers (Leica EMPACT). Substitution was performed at −80 °C in acetone containing 1% OsO_4 and 0.05% uranyl acetate for 58 h. The temperature was then raised to −30 °C within 5 h. The samples were kept at this temperature and in the same medium for 2 h and were subsequently brought to 5 °C within 3.5 h and then to room temperature. After rinsing with acetone, the cells were transferred into propylene oxide and embedded in epoxy resin (Araldite 502/EMBED-812 kit; Electron Microscopy Sciences, Ft. Washington, Pa., U.S.A.). For immunocytochemical studies, cells were transferred into ethanol after the rinsing step with acetone and embedded in LR White Resin (London Resin Company Ltd, Theale, England).

Ultrathin sections with a maximum thickness of about 50 nm or thick sections (approximately 140 nm) were cut on a Reichert Ultracut E (Reichert AG, Vienna, Austria) and were mounted on uncoated copper or gold grids with narrow hexagonal mesh. For immunocytochemical labelling a primary antibody against *M. denticulata* mucilage and a secondary antibody (G-7652) labeled with gold (diameter, 10 nm) was applied to 50 nm thick sections (for further details, see Lütz-Meindl and Brosch-Salomon 2000, Holzinger et al. 2000; A. Oertel, N. Aichinger, R. Hochreiter, J. Thalhamer, U. Lütz-Meindl, University of Salzburg, unpubl.). Micrographs of unstained sections at CTEM or elastic bright-field mode or filtered at an energy range of 250 eV (energy window, 20 eV) below the carbon K edge (high-contrast images, HCI) were taken at a LEO 912 TEM (LEO Electron Microscopy, Oberkochen, Federal Republic of Germany) with in-column energy filter (Ω filter; Uhlemann and Rose 1996, Kujawa and Krahl 1998) operated with a LaB6 cathode and an acceleration voltage of 80 kV. For the HCI mode an illumination angle between 1.6 and 2 mrad and an exposure time of 5 to 10 s was used. Images filtered at zero-loss energy were defocused to obtain phase contrast, whereas HCIs were taken at Gaussian focus. Images were captured by either a Proscan slow-scan charge-coupled-device camera run by the BioVision/VarioVision 3.2 (SIS, Soft Imaging System, Münster, Federal Republic of Germany) software or a Gatan (Munich, Federal Republic of Germany) digital slow-scan camera and a Gatan digital micrograph software for processing.

Results

Unstained 50 nm thick sections of either cryo- or chemically fixed *M. denticulata* cells reveal low contrast in CTEM (Fig. 1a). Organelles and vesicles are only weakly outlined against their cytoplasmic background. Because of the thinness of the sections, membranes are frequently not depicted as continuous lines but appear disintegrate and are hard to discriminate from the background. Delicate structures in the cytoplasm with only low electron scattering abilities or interconnections between organelles are not visible. When inserting the slit aperture to eliminate inelastically scattered electrons (elastic bright field filtered

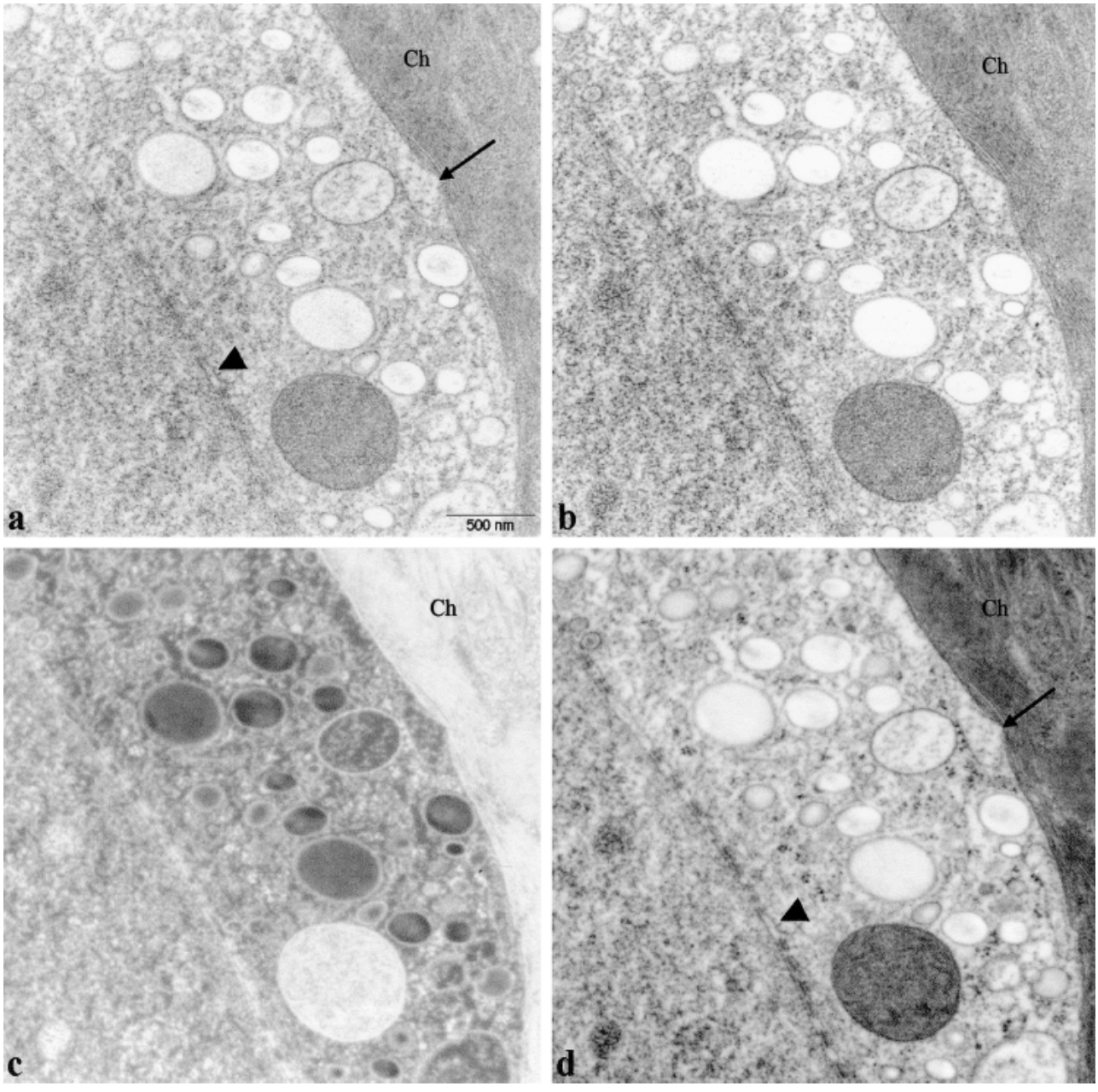

Fig. 1a–d. Nuclear area of a high-pressure-frozen and cryosubstituted nongrowing *M. denticulata* cell. 50 nm thick section, unstained. **a** Unfiltered CTEM image with low contrast. ER cisternae (arrow) and nuclear membrane (arrowhead) hardly visible. **b** Elastic bright field filtered at zero-loss energy, general contrast slightly increased. **c** HCI, filtered below the carbon-specific absorption edge (250 eV; energy window, 20 eV). **d** Same image as in **c**, inverted to "normal" contrast mode by processing. Vesicles, ER cisternae (arrow) in contact with chloroplast (*Ch*) and nuclear membrane (arrowhead) clearly visible

at zero-loss energy) the "positive contrast" in general increases (Fig. 1b). Membranes appear darker and more distinct, yet still valuable structural information is hidden due to the low differences between organelles and vesicles and the cytoplasmic background.

Images filtered in an energy range of 250 eV below the carbon-specific absorption edge appear in "negative contrast" (Figs. 1c and 2a) but can be easily brought to the usual contrast mode by digital processing (Fig. 1d). HCIs are clearly superior to images taken by CTEM or by elastic bright-field mode in both contrast and structure information (compare Fig. 1a with d, Fig. 2c with d, Fig. 3a with b, Fig. 3c with d, Fig. 3e with f, and Fig. 4a with b). Poststaining of sections with heavy metals can be omitted

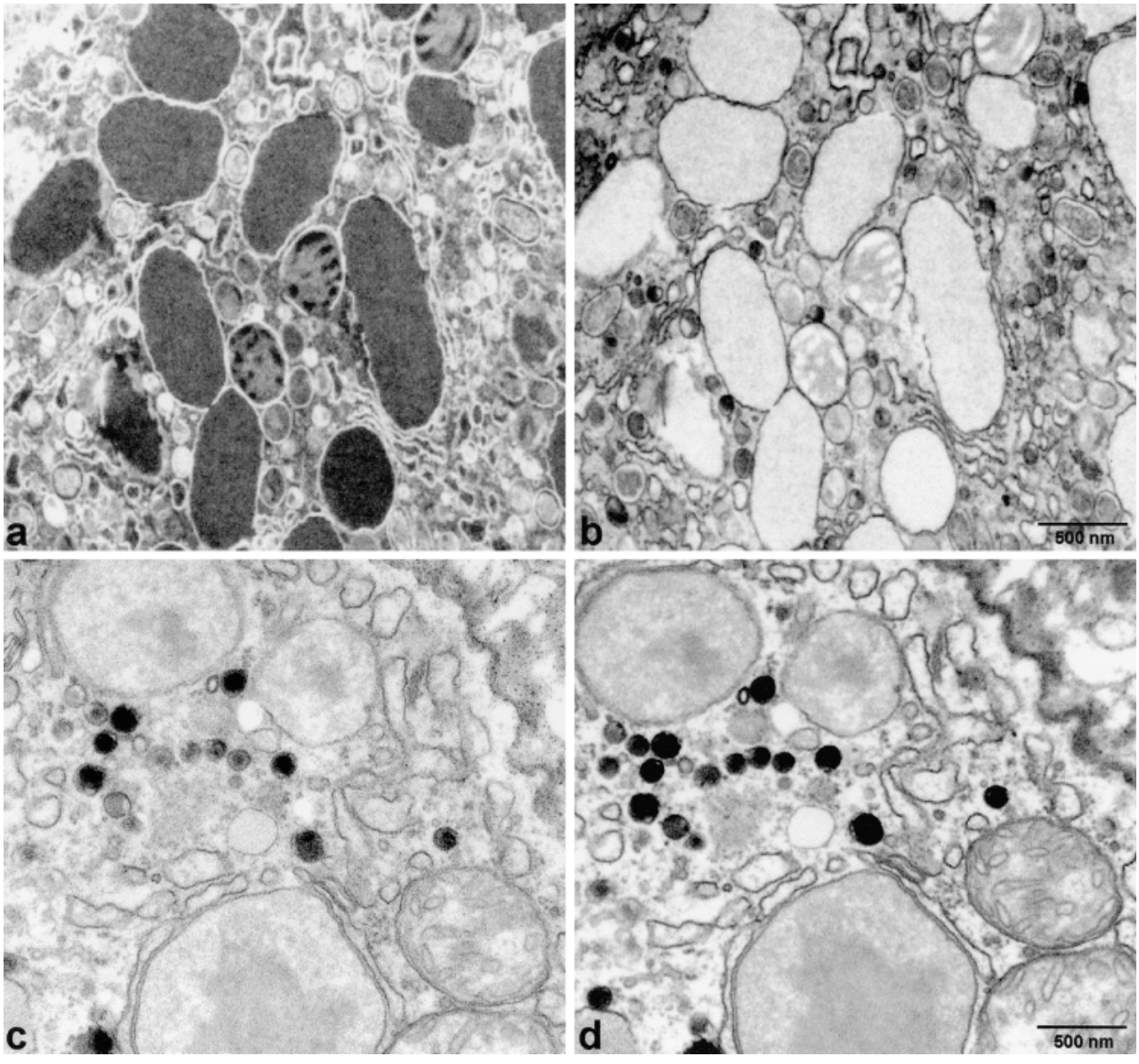

Fig. 2a–d. Different vesicle populations in a growing, chemically fixed *M. denticulata* cell. 50 nm thick section, unstained. **a** and **b** Micrographs taken by EFTEM technique below the carbon-specific absorption edge (250 eV; energy window, 20 eV); **b** image inverted by processing. **c** Elastic bright field filtered at zero-loss energy. **d** HCI of the same area, filtered below the carbon-specific absorption edge (250 eV; energy window, 20 eV). Vesicle contents and membranes clearly visible

when using HCI mode. Organelles and vesicles are clearly distinguishable from the background (Figs. 1d and 2b, d) and so are weakly contrasted cell walls from the surrounding embedding medium (Fig. 3d, f). Membranes such as the nuclear membrane (Fig. 1d), dictyosomal cisternae or the trans-Golgi network (Fig. 3b) are clearly outlined. Differences in the contents of secretory vesicles (Fig. 2c, d) and vacuoles (Fig. 3c, d) become visible. Delicate structures like endoplasmic reticulum (ER) cisternae in contact with the chloroplast (Fig. 1a, d) and with the plasma membrane (Fig. 3c, d) or connecting two adjacent mitochondria (Fig. 3e, f) are distinctly delineated. Organelle interactions such as product transfer between mucilage vesicles (Fig. 3a, b) or the discharge of a mucilage vesicle into a lysosome as shown in Fig. 4a and b reveal more details when energy filtering below the carbon-specific absorption edge is employed. For example, in Fig. 4b it becomes clear that small droplets of mucilage are in contact with the lysosome at two particular sites where the membrane of the vesicle has opened.

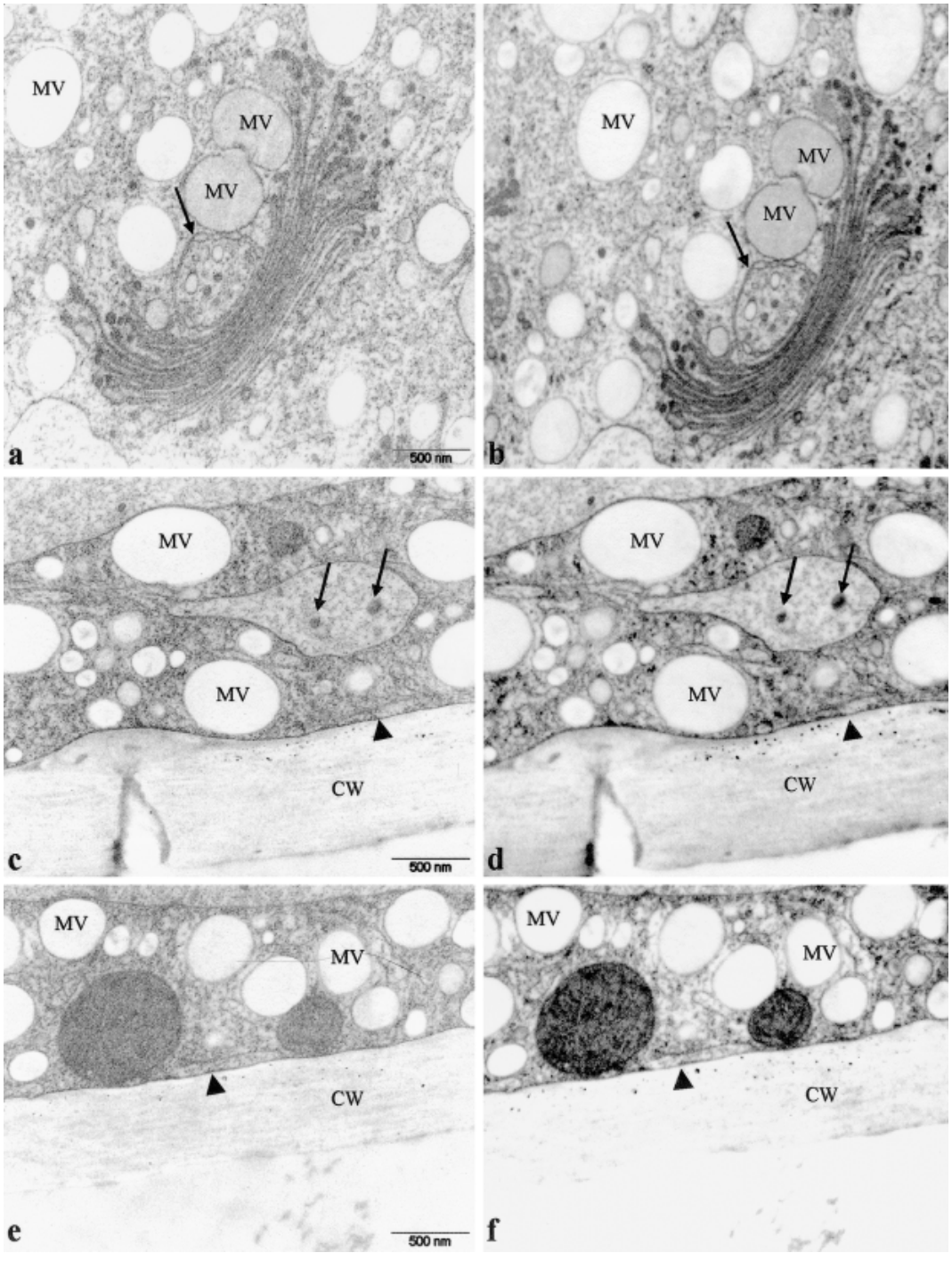

Fig. 3a–f. Different cytoplasmic areas of high-pressure-frozen and cryosubstituted nongrowing *M. denticulata* cells. 50 nm thick sections, unstained. **a**, **c**, and **e** Elastic bright field filtered at zero-loss energy. **b**, **d**, and **f** HCIs, filtered below the carbon-specific absorption edge (250 eV; energy window, 20 eV). **a** and **b** Dictyosome with mucilage vesicles (*MV*) of different developmental stages and trans-Golgi-network (arrow). **c** and **d** Different vesicle populations, ER cisterna and a vacuole. Vacuole contents (arrows), ribosomes, and cortical ER cisterna (arrowhead) much better visible in **d**. **e** and **f** Mucilage vesicles (*MV*) and mitochondria connected by an ER cisterna (arrowhead). Structural information and contrast much better in **f**

Vesicular structures almost not detectable in elastic bright-field mode appear as distinct bodies (compare Fig. 4a with b).

When thick sections (140 nm) are used for TEM investigations, the background noise impedes visualization of structural details in CTEM and also in elastic bright-field

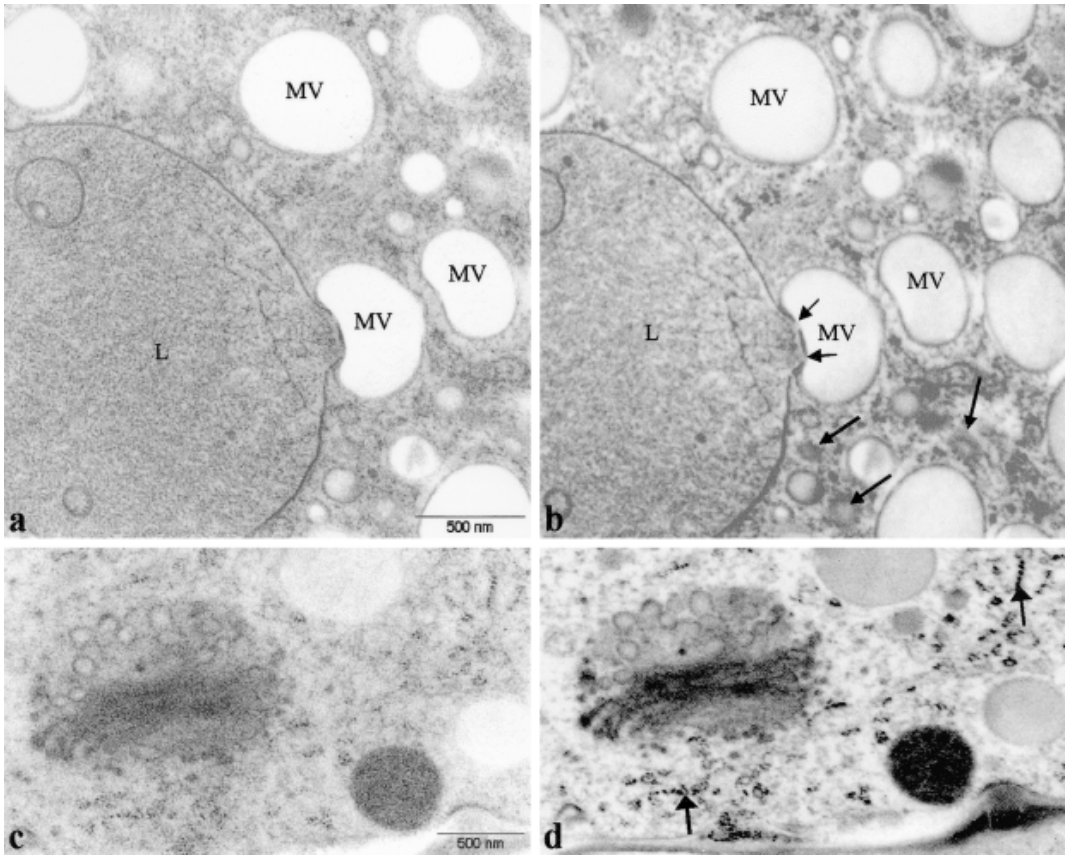

Fig. 4. **a** and **b** Material transfer between a lysosome (*L*) and a mucilage vesicle (*MV*). High-pressure freeze fixation and cryosubstitution. 50 nm thick section, unstained. **a** Elastic bright field filtered at zero-loss energy. **b** HCI, filtered below the carbon-specific absorption edge (250 eV; energy window, 20 eV). Mucilage droplets (short arrows) in contact with the lysosome and vesicular structures in the cytoplasm (long arrow) visible only in **b**. **c** and **d** Thick section (140 nm) of a high-pressure frozen and cryosubstituted *M. denticulata* cell. **c** Elastic bright field filtered at zero-loss energy. **d** HCI, filtered below the carbon-specific absorption edge (250 eV; energy window, 20 eV). Structure of dictyosome and ribosomes (arrows) more distinct in **d**

mode (Fig. 4c), whereas the EFTEM image filtered at about 250 eV provides clearer structural information (Fig. 4d).

Employment of EFTEM below the carbon-specific absorption edge is also suitable for immunoelectron microscopy as immunomarkers such as gold particles are clearly visible in HCIs. In addition, the structures at which the antigens are located show sufficient contrast for a detailed assignment without heavy metal poststaining (Fig. 5a–d).

In general, images taken below the carbon-specific absorption edge appear in a different focus mode when compared to images from CTEM where phase contrast is employed for focussing. This means that HCIs produce a more "three-dimensional" impression and appear less sharp, though providing more structural information. Problems which may arise when using the EFTEM mode essentially encompass instabilities of the specimen in the electron beam at the high illumination angle of about 2 mrad required to obtain sufficient signal. In this respect epoxy resins have proved to be more stable than London resins (LR White), which frequently require preexposure to a low-dose illumination before capturing images.

Discussion

The present study demonstrates the advantages of using EFTEM below the carbon-specific absorption edge for routine structural analysis of plant cells and for immunoelectron microscopy in comparison with the employment of CTEM or filtering at elastic bright field. With an in-column spectrometer for image generation at an energy loss of about 250 eV, poststaining with uranyl acetate and lead citrate, indispensable for CTEM, is no longer required. On the one hand, this means that specimen preparation for TEM becomes faster and contaminations by heavy metals are avoided. On the other hand, the information on ultra-

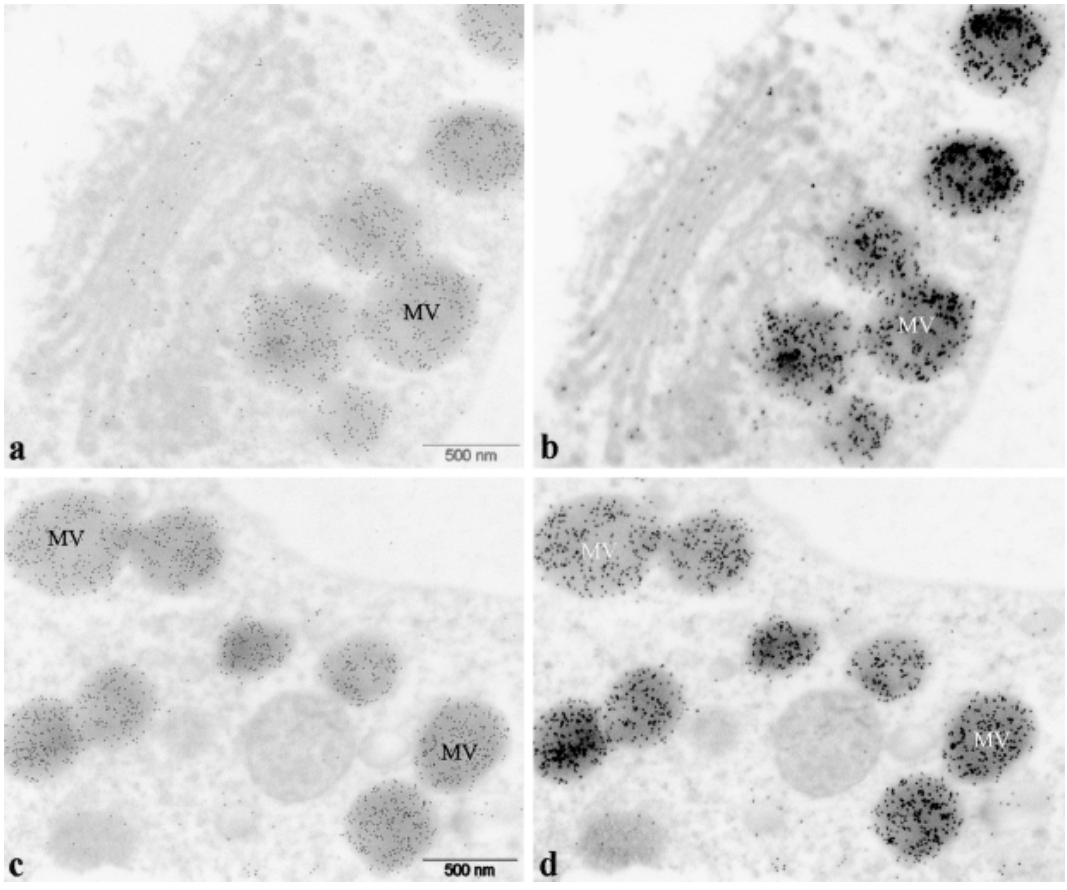

Fig. 5a–d. Immunogold labelling of dictyosome and vesicles with primary antibody against *M. denticulata* mucilage. Mucilage vesicles labelled with 10 nm gold particles. High-pressure freeze fixation and cryosubstitution, 50 nm thick section, unstained. **a** and **c** Elastic bright-field mode filtered at zero-loss energy. **b** and **d** HCI, filtered below the carbon-specific absorption edge (250 eV; energy window, 20 eV)

structure obtained is more accurate than with the relatively unspecific heavy metal staining which may cover details (Carlemalm et al. 1985). This is particularly advantageous when studying filamentous or membranous connections or interactions between organelles. Also the contents of secretory vesicles and other vesicular structures become visible often only when EFTEM is used. The images obtained are more reliable than those produced by CTEM as they are independent of the nature and concentration of the heavy metals used for preparation and staining and reveal the "real" biological structure. In addition, EFTEM below the carbon-specific absorption edge provides an element-specific contrast and the micrographs may yield information on the chemical composition of the structures investigated. This prevents misinterpretations which may occur in CTEM when cellular constituents of different chemical nature are described as the same structures only because of similarities in their morphological appearance. With a corresponding software for element mapping, the EFTEM technique used in the present study can be extended to an analytical method for the detection of specific elements in intracellular compartments and electron energy loss spectra can be obtained (Ochs et al. 1994, 2001; Vázquez-Nin et al. 1998; Mondi et al. 2002).

The use of very thin (50 nm or less) sections for EFTEM below the carbon-specific absorption edge offers better spatial resolution than the 80 to 100 nm sections in bright-field CTEM at a particular acceleration voltage. Structures of HCIs are much more clearly defined than those obtained from dark-field CTEM which was the only technique for imaging very thin unstained sections before the introduction of EFTEM (Carlemalm et al. 1985). Thin sections investigated by EFTEM allow better and more accurate assignment of the antibody to the antigen. Detection and localization of immunomarkers such as gold particles at cellular compartments is easier as both the marker and the biological structure reveal sufficient contrast.

When using thick sections, as required for stereological quantification and visualization of three-dimensional intracellular organization (Körtje et al. 1996), the chromatic error is avoided in EFTEM and the resulting images reveal high resolution and contrast.

In summary, EFTEM at an energy loss of about 250 eV has proved to be a powerful tool for ultrastructural analysis of plant cells. HCIs are superior to images taken by CTEM and to zero-loss filtering both in contrast generation and in providing structural information. The technical problems arising from the use of EFTEM, such as the requirement of 50 nm thick sections or instabilities of the specimen due to high illumination by the electron beam, are comparably minor and can be neglected in routine use of this technique.

Acknowledgments

We thank Adolf Ellinger and Margit Pavelka (Institute of Histology and Embryology, University of Vienna) for providing access to their Balzers hyperbaric freezer and the Leica company for making the Leica EMPACT high-pressure freezer available for testing purposes. The study has been supported by the Austrian Science Fund, project P15849 to U.L.-M.

References

Angert I, Majorovits E, Schröder RR (2000) Zero-loss image formation and modified contrast transfer. Ultramicroscopy 81: 203–222

Carlemalm E, Colliex C, Kellenberger E (1985) Contrast formation in electron microscopy of biological material. Adv Electron Electron Phys 63: 269–334

Heinrich U-R, Maurer J, Koesling D, Mann W, Förtermann U (2000) Immuno-electron microscopic localization of the α1- and β1-subunits of soluble guanylyl cyclase in the guinea pig organ of Corti. Brain Res 885: 6–13

Hofer F, Pabst M (1998) Characterization of deposits in human lung tissue by a combination of different methods of analytical electron microscopy. Micron 29: 7–15

Holzinger A, Meindl U (1997) Jasplakinolide, a novel actin targeting peptide, inhibits cell growth and induces actin filament polymerization in the green alga *Micrasterias*. Cell Motil Cytoskeleton 38: 365–372

– Valenta R, Lütz-Meindl U (2000) Profilin is localized in the nucleus-associated microtubule and actin system and is evenly distributed in the cytoplasm of the green alga *Micrasterias denticulata*. Protoplasma 212: 197–205

Hoshi K, Ejiri S, Probst W, Kamino T, Yaguchi T, Yamahira N, Ozawa H (2001) Observation of human dentine by focused ion beam and energy filtering transmission electron microscopy. J Microsc 201: 44–49

Kiermayer O (1968) The distribution of microtubules in differentiating cells of *Micrasterias denticulata*. Planta 83: 223–236

Körtje K-H, Paulus U, Ibsch M, Rahmann H (1996) Imaging of thick sections of nervous tissue with energy-filtering transmission electron microscopy. J Microsc 183: 89–101

Kujawa S, Krahl D (1998) Comparison between A-type and B-type imaging Ω energy filters. In: International Conference on Electron Microscopy, Cancun, Mexico, 1998, Symposium E, vol 1, pp 241–242

Leapman RD, Hunt JA, Buchanan RA, Andrews SB (1993) Measurement of low calcium concentrations in cryosectioned cells by parallel-EELS mapping. Ultramicroscopy 49: 225–234

Lechaire J-P, Shillito B, Frébourg G, Gaill F (2002) Elemental characterisation of microorganism granules by EFTEM in the tube wall of a deep-sea vent invertebrate. Biol Cell 94: 243–249

Lütz-Meindl U, Brosch-Salomon S (2000) Cell wall secretion in the green alga *Micrasterias*. J Microsc 198: 208–217

Meindl U (1990) Effects of temperature on cytomorphogenesis and ultrastructure of *Micrasterias denticulata* Bréb. Protoplasma 157: 3–18

– (1993) *Micrasterias* cells as a model system for research on morphogenesis. Microbiol Rev 57: 415–433

– Lancelle S, Hepler PK (1992) Vesicle production and fusion during lobe formation in *Micrasterias* visualized by high-pressure freeze fixation. Protoplasma 170: 104–114

Mondi C, Leifer K, Mavrocordatos D, Perret D (2002) Analytical electron microscopy as a tool for accessing colloid formation process in natural waters. J Microsc 207: 180–190

Ochs M, Fehrenbach H, Richter J (1994) Electron spectroscopic imaging (ESI) and electron energy loss spectroscopy (EELS) of multilamellar bodies and multilamellar body-like structures in tannic acid-treated alveolar septal cells. J Histochem Cytochem 42: 805–809

– – – (2001) Ultrastructure of canine type II pneumocytes during hypothermic ischemia of the lung: a study by means of conventional and energy filtering transmission electron microscopy and stereology. Anat Rec 263: 118–126

Oertel A, Holzinger A, Lütz Meindl U (2003) Involvement of myosin in intracellular motility and cytomorphogenesis in *Micrasterias*. Cell Biol Int 27: 977–986

Reimer L (1995) Electron spectroscopic imaging. In: Reimer L (ed) Energy-filtering transmission electron microscopy. Springer, Berlin Heidelberg New York, pp 347–393

– Rennekamp R, Fromm I, Langenfeld M (1990) Contrast in the electron spectroscopic imaging mode of a TEM. J Microsc 162: 3–14

Schlösser UG (1982) Sammlung von Algenkulturen. Ber Deutsch Bot Ges 95: 181–276

Stegmann H, Wepf R, Schröder RR, Fink RHA (1999) Quantification of total calcium in terminal cisternae of skinned muscle fibers by imaging electron energy-loss spectroscopy. J Muscle Res Cell Motil 20: 505–515

Uhlemann S, Rose H (1996) Acceptance of imaging energy filters. Ultramicroscopy 63: 161–167

Vannier-Santos MA, Lins U (2001) Cytochemical techniques and energy-filtering transmission electron microscopy applied to the study of parasitic protozoa. Biol Proced Online 4(3): 8–18

Vázquez-Nin GH, Echeverria O, Abolhassani-Dadras S, Boutinard-Rouelle-Rossier V, Fakan S (1998) Electron filtering transmission electron microscopical analysis as a tool for the study of the relationships between structure, composition and function of ribonucleoproteic particles. In: International Conference on Electron Microscopy, Cancun, Mexico, 1998, Symposium O, vol 1, pp 691–693